Tropospheric Mean Temperature and Its Relationship to the Oceans and Atmospheric Aerosols

ALFREDO R. NAVATO, REGINALD E. NEWELL, JANE C. HSIUNG AND CLARE B. BILLING, JR.

Department of Meteorology, Massachusetts Institute of Technology, Cambridge 02139

BRYAN C. WEARE

Department of Land, Air and Water Resources, University of California, Davis, CA 95616

(Manuscript received 20 October 1978; in final form 17 April 1980)

ABSTRACT

Multiple-regression analyses of changes in tropospheric mean temperature as predictands and Pacific, Atlantic and Indian Ocean sea surface temperatures and atmospheric aerosol concentrations as predictors show that large fractions of the variances of the tropical, Northern Hemispheric and Southern Hemispheric extratropical tropospheric temperatures may be explained by fluctuations in ocean surface temperatures and atmospheric aerosols. The sensitivity of the tropical, Northern Hemisphere and Southern Hemisphere extratropical tropospheric temperatures to the various predictors are estimated.

To improve the precision of the estimates in the presence of serial correlations in the variables we used a generalized least-squares procedure to obtain the regression models.

1. Introduction

It has previously been reported by Newell and Weare (1976) that changes in the seasonal mean temperature of the tropical troposphere are related to changes in the sea surface temperature (SST) of the Pacific and to changes in atmospheric transmission due to volcanic activity. They found no dependence on changes in Atlantic SST's. We report here an extension of this work to include SST's from the Indian Ocean and aerosol data from the extratropical Southern Hemisphere. Using a multiple-regression model of the air-sea-aerosol interaction, we estimated the sensitivity of tropical, extratropical Northern Hemisphere and extratropical Southern Hemisphere tropospheric temperatures to the SST's of the individual oceans and to the atmospheric aerosol concentrations over the northern tropics and over the extratropical Southern Hemisphere. Whereas sea surface temperature patterns were previously characterized by the results of an empirical orthogonal function (EOF) analysis of unnormalized data for each ocean, in this study we include results for the analyses of normalized data (see Section 2 for a discussion of normalized and unnormalized analyses). We now find that the EOF's based on normalized data for the Atlantic Ocean and for the Indian Ocean are also important. Allowing a predictor for each one of the three oceans and for each of the two aerosol indices, we assumed five predictors for each regression equation. We found that in the years 1958–72 corresponding to the period of overlap for all our time series, up to 50.2% of the variance of the tropical tropospheric mean temperatures, 21.8% of the variance of the extratropical Northern Hemisphere tropospheric temperatures, and 21.8% of the variance of the extratropical Southern Hemisphere tropospheric temperatures can be explained by these five predictors. As will be outlined later, these findings are broadly in agreement with earlier work by Walker (1923, 1924) on the interrelationship between sea and air temperature and pressure gradient changes.

When the SST and the aerosol time series are used as predictors, the time lags of those predictors which yield the maximum explanation of variance of tropospheric temperatures contribute evidence toward answering the question: Does the atmosphere drive the ocean, or is it the other way around?

2. Data and procedures

We developed a multiple-regression model with nonseasonal anomalies of monthly tropospheric mean temperature [i.e., departures from long-term (1958–72) means for each calendar month] as dependent variable (predictand) and nonseasonal anomalies of monthly mean sea surface temperature (from 1949–72 means for the Atlantic and Indian Oceans, from 1949–76 means for the Pacific Ocean) and stratospheric aerosol at appropriate lags as independent variables (predictors). Fig. 1 shows the time series

0027-0644/81/020244-11$06.75

used, and Fig. 2 their corresponding autocorrelation functions.

To represent tropospheric mean temperature we followed Angell and Korshover (1975) and made use of the 700–300 mb geopotential height difference. The stations used are listed in Table 1. We omitted stations used by Angell and Korshover for which there were significant gaps in the record. Our data were derived entirely from observations in *Monthly Climatic Data for the World* (NOAA, 1958–78). The tropical temperature was characterized by averaging geopotential height differences for a number of stations near latitudes 20°N and 20°S. Nonseasonal anomalies averaged over stations on opposite sides of the equator showed a positive correlation of 0.459. For middle and high latitudes it is more difficult to characterize variations by a single temperature because of the importance of large-scale standing waves. To check for data errors, the time series for each station was examined for unusually abrupt or large changes and such data were compared where possible with adjacent station values, taking spatial continuity of the lapse rates into account. Rejected data and missing values were filled in by linear interpolation. Finally, the station data were combined to produce one time series for each zone—the tropics, the extratropical Northern Hemisphere and the extratropical Southern Hemisphere.

To characterize the patterns of month-to-month SST changes we used an EOF analysis such as has been described by Kutzbach (1967). We performed the analysis separately for each ocean to limit the size of the matrices to be manipulated. We began with 368 5° × 5° grid squares to represent the Pacific Ocean. Where data were sparse, we compounded these squares into 10° longitude by 5° latitude grid rectangles, which resulted in 250 grid points on which we performed an EOF analysis. The Atlantic Ocean EOF analysis was based on 250 5° × 5° grid squares. The Indian Ocean was represented by 121 5° × 5° grid squares. Data were available for 1949–78 for the Pacific and 1949–72 for the Atlantic and Indian Oceans. Results for the Pacific for 1949–73 and for the Atlantic for 1949–69 have been reported earlier by Weare *et al.* (1976) and Weare (1977), respectively. These published results were for the unnormalized deviations. All these were rerun for the present study after a careful checking of each grid point, using an approach similar to that used for the air temperatures. Some differences were found, e.g., where a zero line runs along 60°N from 20°W to 40°W in Fig. 7 of Weare's (1977) Atlantic (unnormalized) EOF, we now have high values for the corresponding EOF in that area (see our Fig. 4). Furthermore, the analysis for the Pacific Ocean was extended to 30°S. The spatial patterns of the eigenfunctions which explain the largest fraction of the variance (the first mode) of the Pacific Ocean SST's shown in Fig. 3, the Atlantic Ocean SST's shown in Fig. 4 (unnormalized mode) and Fig. 5 (normalized mode), and the Indian Ocean SST's shown in Fig. 6, have not been published elsewhere. Eigenfunctions computed for a more limited area of the Indian Ocean have been used by Weare (1979) in a study related to the Indian monsoon. Maps of the long-term mean sea surface temperatures representative of summer and winter and the standard deviations for winter based on the same data set have been published earlier by Newell *et al.* (1978).

The basic difference between the normalized and unnormalized results is due to the fact that the separate physical phenomena which dominate the variations, such as the Gulf Stream or equatorial upwelling, are given different weights in computing the eigenfunctions. In the unnormalized EOF analysis, regions which have large coherent variability for relatively long periods tend to show up as regions of large absolute values of the EOF's in one or more of the first few principal modes. In the corresponding normalized analysis, since the data have been normalized by dividing by the standard deviation, the contribution to the EOF's by those large variance regions are reduced. Consequently, high-variance regions which showed up prominently in the unnormalized analysis may no longer dominate the normalized analysis.

The time series for the principal EOF modes used in this investigation are included in Fig. 1. The time series corresponding to the first mode of the unnormalized nonseasonal EOF for the Pacific Ocean (which explains 18.4% of the variance) resulted from an analysis by Billing (1979) of the Pacific Ocean SST data set updated to include December 1978. The variability for the Pacific is mainly contributed by the equatorial regions and by an area in the North Pacific in the eastern sector. A positive value in the time series represents warm anomalies in these two areas.

The principal unnormalized mode shown for the Atlantic Ocean represents 10.4% of the variance (Hsiung, 1978). A positive value in the corresponding time series represents warm anomalies from about 5°N to 40°S, warm anomalies between 20 and 30°N, the eastern edges of the Atlantic from 30 to 70°N up to the North Sea, and strong cold anomalies in the central and western Atlantic from about 30 to 70°N. For the normalized EOF's we divided the anomalies by the standard deviation taken over the entire period covered by the data. For the mode shown in Fig. 5, a positive value in the time series represents cold anomalies in the central 30–50°N region, and large warm anomalies around 20°N, off Scotland, near the equator, and off Southwest Africa.

The principal unnormalized mode for the Indian Ocean SST's (not shown) represents 11.0% of the total variance of the Indian Ocean. The correspond-

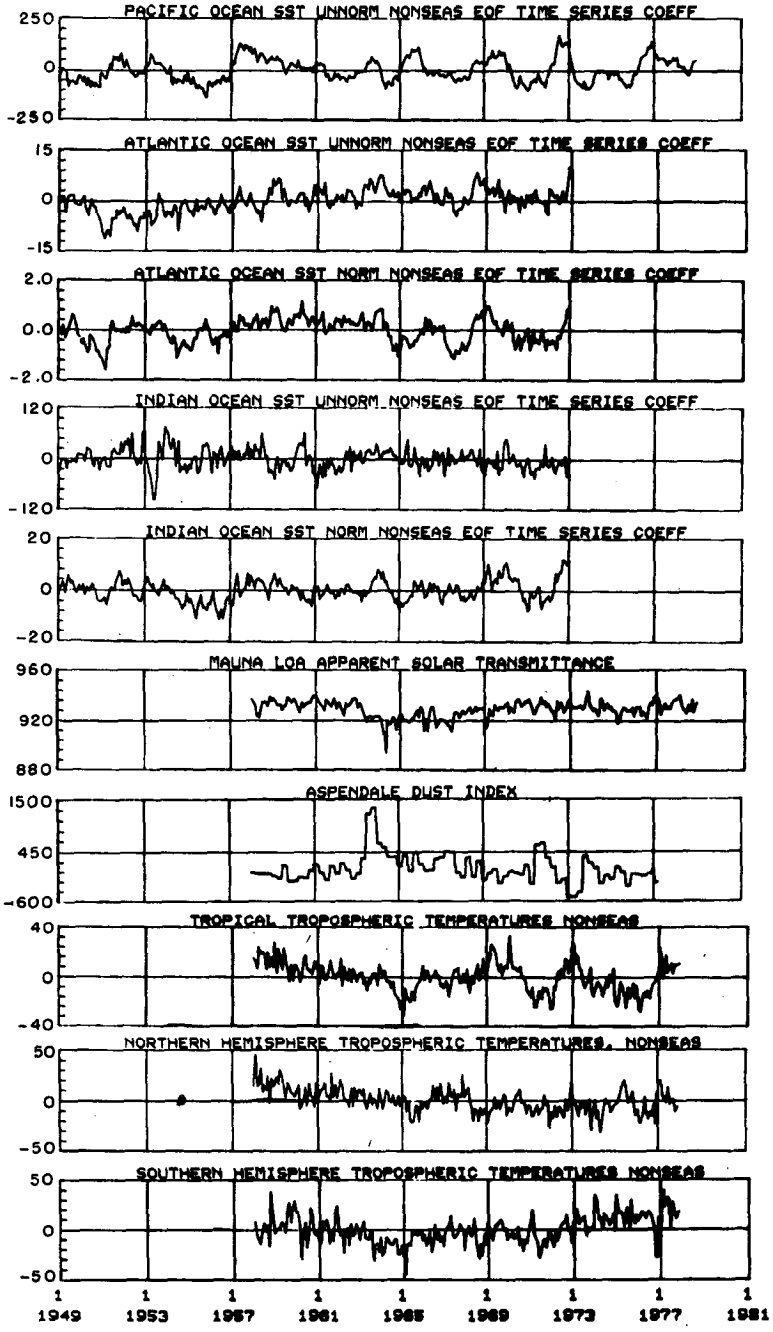

FIG. 1. Time series representations of sea surface temperature anomalies (top five curves), of atmospheric aerosols (sixth and seventh curves), and of nonseasonal monthly mean tropospheric temperatures (bottom three curves). The scales along the left border are relative scales. The first curve (P) is the time series coefficient of the first principal component of the unnormalized nonseasonal empirical orthogonal function (EOF) representation of the Pacific sea surface temperature anomalies. The anomalies are taken with respect to the 1949–76 mean temperature for each calendar month for each 5° × 5° grid square. The second curve (AU) is the time series coefficient of the principal component of the unnormalized nonseasonal Atlantic EOF. The 1949–69 EOF spatial pattern and the 1970–72 anomalies were used to extend the two Atlantic time series coefficients from 1969 to 1972. The third curve (A) is the time series coefficient of the principal component of the normalized nonseasonal Atlantic EOF's. The normalization was done by dividing the anomalies by the standard deviation for each 5° × 5° grid square. The time series coefficients of the principal component of the unnormalized nonseasonal Indian Ocean EOF's are shown as the fourth curve. The fifth curve (I) is the time series coefficient of the principal component of the

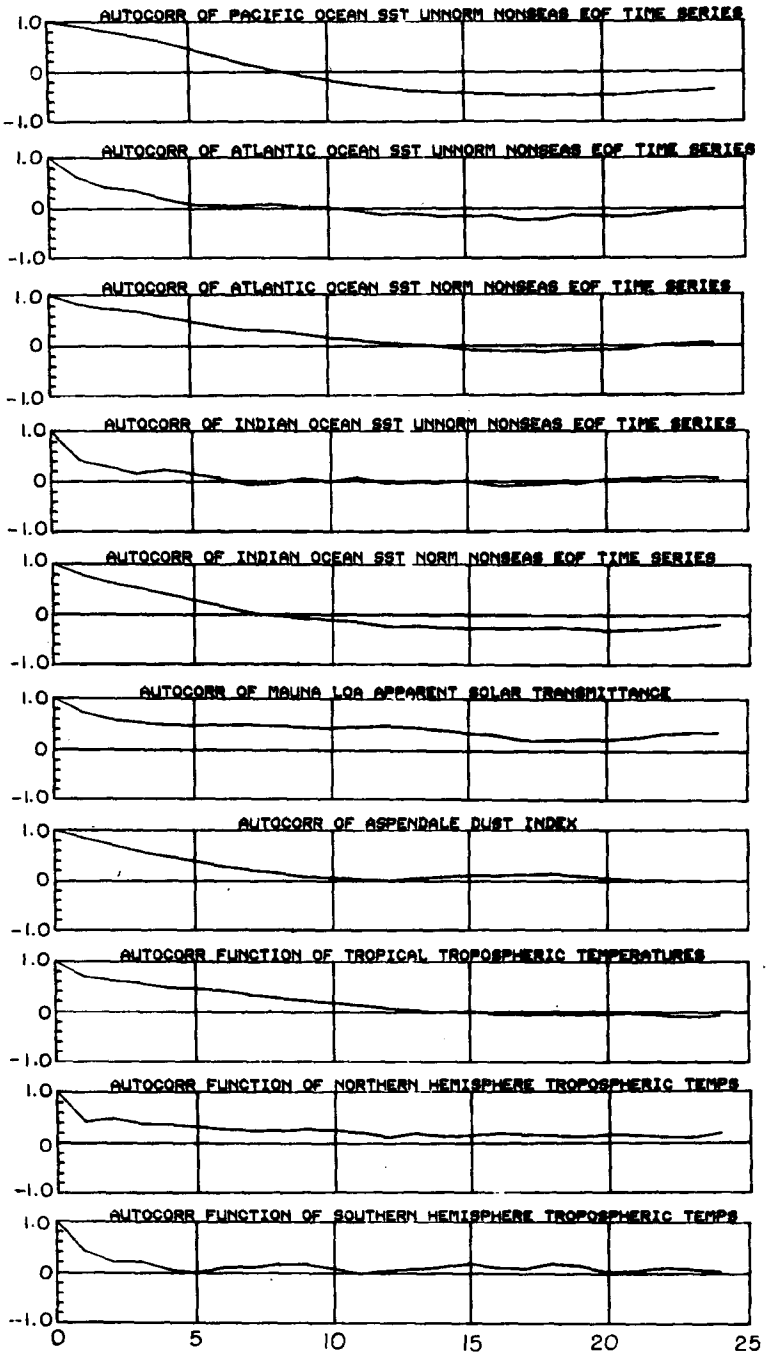

FIG. 2. Autocorrelation functions of each of the time series shown in Fig. 1, in the same order, from 0 to 24 months lag.

normalized nonseasonal Indian Ocean EOF's. It was normalized by the standard deviation for each calendar month. The sixth curve (M) is the apparent solar transmittance which is proportional to aerosol concentrations over Mauna Loa. The seventh curve (AD) is proportional to the seasonal Aspendale dust index. Note that a high transmittance corresponds to a lower dust index. TTT is the nonseasonal monthly mean tropical tropospheric temperature shown as the eighth curve. The nonseasonal mean Northern Hemisphere extratropical tropospheric temperature (NTT) is shown as the ninth curve. STT is the nonseasonal monthly mean Southern Hemisphere tropospheric temperature shown as the last curve.

TABLE 1. Upper air stations.

Name	Latitude	Longitude
Tropical stations (between 20°N and 20°S)		
Pt. Hedland	20.23°S	118.37°E
Wake Island	19.17°N	166.39°E
Nandi	17.45°S	177.27°E
Hilo	19.43°N	155.04°W
San Juan	18.26°N	66.0°W
Dakar	14.44°N	17.3°W
Khartoum	15.36°N	32.33°E
Northern Hemisphere Stations (above 20°N)		
Brownsville	25.54°N	97.26°W
Calcutta	22.39°N	88.27°E
Kirensk	57.46°N	108.07°E
Wakkanai	45.25°N	141.41°E
St. Paul	57.09°N	170.13°W
Ship P	50.00°N	145.0°W
Great Falls	47.29°N	111.22°W
Moosonee	51.16°N	80.39°W
Ship B	56.5°N	50.9°W
Ship J	52.5°N	20.0°W
Uccle	50.48°N	4.21°E
Kiev	50.24°N	30.27°E
Omsk	54.56°N	73.24°E
Pt. Barrow	71.18°N	156.47°W
Mould Bay	76.14°N	119.20°W
Alert	82.30°N	62.20°W
Jan Mayen	70.56°N	8.40°W
Southern Hemisphere Stations (below 20°S)		
Chatham Island	44.0°S	176.6°W
Marion Island	46.53°S	37.52°E
Wilkes/Casey	66.15°S	110.32°E
Amundson Scott	90.00°S	0.0°W
Adelaide	34.57°S	138.32°E
Antofogasto	23.22°S	70.28°W
Puerto Montt	41.5°S	72.9°W
Gough Island	40.21°S	9.53°W
New Amsterdam	37.8°S	77.6°E
Mawson	67.36°S	62.53°E

ing principal normalized mode shown in Fig. 6 represents 13.8% of the variance. For this new analysis, we supplemented the British Meteorological Office data used by Weare (1979) with data from the Royal Netherlands Meteorological Institute (1976) and from the *Meteorological Atlas of the International Indian Ocean Expedition* compiled by Ramage *et al.* (1972). For the normalized EOF's for the Indian Ocean, we divided the anomalies from the seasonal cycles by the long-term monthly standard deviation of these anomalies at each grid square. In the Indian Ocean a positive value in the time series represents warm anomalies in the entire region north of 30°S, particularly north of the equator, and cold anomalies between 55 and 75°E south of 30°S, at the northern edge of the "roaring forties."

To represent aerosol we used two indices: the apparent solar transmittance at Mauna Loa, at 19°N latitude (see Pueschel *et al.*, 1972) kindly provided to us by the National Oceanic and Atmospheric Administration (private communication) on a monthly basis from January 1958 to November 1978, and the Aspendale dust index computed by Dyer (1974), which was computed seasonally by Dyer for the period from January 1958 to March 1977.

From physical considerations, we decided (*a priori*), as mentioned above, to select one predictor from each of five variables related to tropospheric mean temperatures: three ocean SST's and two aerosol indices. The time series from which we selected predictors for the three regression models are shown in Fig. 1. We chose (*a posteriori*) the lag or lead (relative to the tropospheric temperature time series) which produced the best correlation with the ordinary least square (OLS) residual after the effects of all previously chosen predictors have been removed. The number of candidate lags and leads considered are listed in the row marked NLL under the corresponding regression coefficient in Eqs. (2)–(4). We continued in this fashion until we had included a predictor from each one of our five relevant variables. We obtained an estimate of the level of confidence of the regression coefficients, i.e., the probability that a sample coefficient would be as large as our estimate if the true regression coefficient were zero, taking into account the number of candidate leads and lags that had to be examined to arrive at the lead or lag to be used. The level of confidence based on two-sided hypothesis tests, now corrected for the *a posteriori* selection procedure used, is listed in the row marked prob under each regression coefficient in Eqs. (2)–(4). The standard errors and the Student's t statistics are listed below each regression coefficient in the rows marked st er and t-s, respectively. Our regression models were of the form

$$y = B_0 + B_1x_1 + B_2x_2 + B_3x_3 + B_4x_4 + B_5x_5 + E \quad (1)$$

where

y	predictand
$x_1, x_2, \cdots$	predictors at appropriate lags or leads
B_0	constant
$B_1, B_2, \cdots$	multiple-regression coefficients
E	residual.

When we used an OLS procedure to obtain regression models, we found much serial correlation in the residuals, probably due to the long autocorrelations typical of climatic variables (see Fig. 2). To improve the precision of our estimates in the presence of serial correlation in our variables we used the method of generalized least squares (GLS) to obtain the regression model (see the Appendix).

3. Results

For tropical tropospheric temperatures we obtained the following regression equation, using beta coefficients:

$$TTT_t = 0.293\ P_{t-6} + 0.266\ A_t + 0.306\ I_{t-1} + 0.127\ M_t - 0.152\ AD_{t-2} \quad (2)$$

st er	0.0733	0.0579	0.0664	0.0543	0.0594
t-s	4.24	4.28	4.71	2.09	−2.47
NLL	10	11	11	3	5
prob	0.005	0.006	0.006	0.115	0.078,

where

TTT_t tropical tropospheric temperature at month t

P_{t-6} Pacific Ocean SST unnormalized EOF time series coefficient for month $t - 6$

A_t Atlantic Ocean SST normalized EOF time series coefficient for month t

I_{t-1} Indian Ocean SST normalized EOF time series coefficient for month $t - 1$

M_t Mauna Loa apparent solar transmittance for month t

AD_{t-2} Aspendale dust index for month $t - 2$.

The lead-lag relation between the variables on the left-hand side of the regression equations and those on the right-hand side (the independent variables, or predictors) is given in the subscript of each predictor. For example, six subtracted from t in the subscript for P in Eq. (2) means that the variable P is ahead of (or leads) TTT by six months. An example of a variable behind by four months is P with subscript $t + 4$ in Eq. (3) below.

The right-hand side (the fitted values) of Eq. (2) explains 50.2% of the variance of the left-hand side. All the variables in Eq. (2) above and Eqs. (3) and (4) below are standardized, i.e., they are deviations from their long-term means divided by their long-term standard deviations. The deviations for TTT, P, A and I are nonseasonal. The Durbin-Watson statistic for the GLS residuals of Eq. (2) has the value 1.92 which shows that there is little serial correlation among the residuals. The statistics for Eq. (2) are based on 178 observations (length of the time series). We can see from the correlations (Table 2a) among the variables involved in Eq. (2) that we cannot group the predictors into sets which would be statistically independent of each other. Hence, we cannot partition the 50.2% of variance explained among the individual predictors.

Using notation similar to that of Eq. (2), we found the following regression equation for the Northern Hemisphere extratropical tropospheric temperature (NTT), using beta coefficients:

$$NTT_t = 0.406\ A_{t-9} - 0.262\ P_{t+4} - 0.126\ I_{t-12} - 0.142\ AD_{t-1} - 0.034\ M_{t-9} \quad (3)$$

st er	0.065	0.072	0.074	0.065	0.060
t-s	5.13	−3.26	−1.65	−1.83	−0.44
NLL	18	9	21	6	11
prob	0.009	0.013	0.891	0.374	0.999,

where NTT_t is the Northern Hemisphere extratropical tropospheric temperature at month t.

The right-hand side (the fitted values) of Eq. (3) explains 21.8% of the variance of NTT. The statistics are based on 168 observations. The Durbin-Watson statistic for the GLS residuals of Eq. (3) has a value

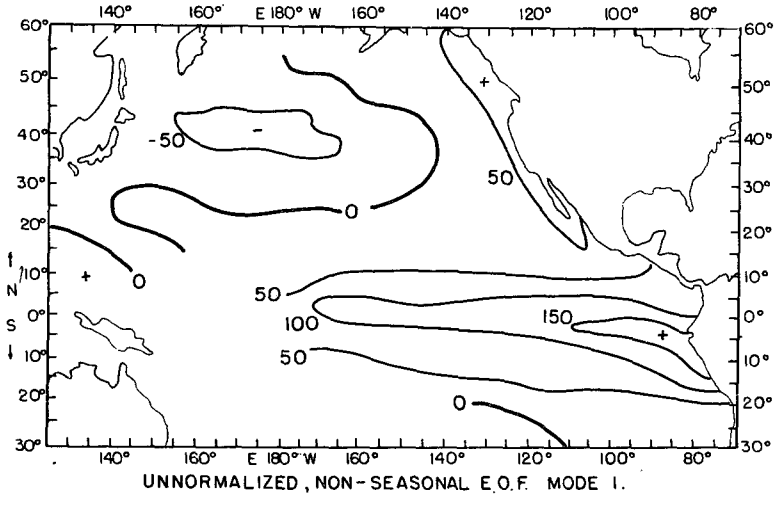

FIG. 3. Spatial pattern of the first principal component (mode 1) EOF representation of Pacific Ocean nonseasonal SST anomalies. The function was multiplied by 1000 to produce an integral scale for the contours.

of 1.84, which shows that there remains no significant serial correlation among these residuals. The correlations among the variables are given in Table 2b.

The regression equation for the Southern Hemisphere extratropical tropospheric temperature (STT), using beta coefficients is

$$STT_t = 305\ M_{t-9} - 0.235\ AU_t + 0.343\ P_{t-2} - 0.186\ AD_t - 0.164\ I_t \quad (4)$$

st er	0.061	0.087	0.090	0.069	0.079
t-s	4.01	−3.14	3.67	−2.33	−1.87
NLL	11	10	7	3	10
prob	0.001	0.020	0.002	0.059	0.495,

where SST_t is the southern hemisphere extratropical tropospheric temperature for month t and AU_t the Atlantic Ocean SST unnormalized EOF time series coefficient for month t.

The right-hand side (the fitted values) of Eq. (4) explains 21.8% of the variance of the left-hand side. The Durbin-Watson statistic for the GLS residuals of Eq. (4) has the value 1.90 which shows that there is little serial correlation among the residuals. The statistics for Eq. (4) are based on 171 observations. The correlations between the variables in regression equation (4) is given in Table 2c.

We found that the GLS residuals for each of the regression equations (2) and (3) have distributions which do not depart significantly from normality. Hence, the estimates of standard errors, statistics, levels of confidence, and fraction of variance explained are reliable (see the Appendix) in the context of asymptotic theory.

The regression coefficients in Eq. (2) give the estimated sensitivity of the tropical tropospheric temperature to oceanic SST's and aerosol concentrations. For example, if it were possible for the Pacific Ocean SST EOF time series to increase by one standard deviation without changing any one of the other predictors in Eq. (2), the tropical tropospheric temperature would increase by 0.293 standard deviations. On the other hand, in Eq. (3), an increase of one standard deviation in the Pacific Ocean SST EOF time series coefficient would follow a 0.262 standard deviation decrease in Northern Hemisphere extratropical tropospheric temperature. The other coefficients, and Eq. (4), may be interpreted in like manner. It may be noted from Table 2 that since the variables are intercorrelated, a change in one usually is accompanied by a change in others as well.

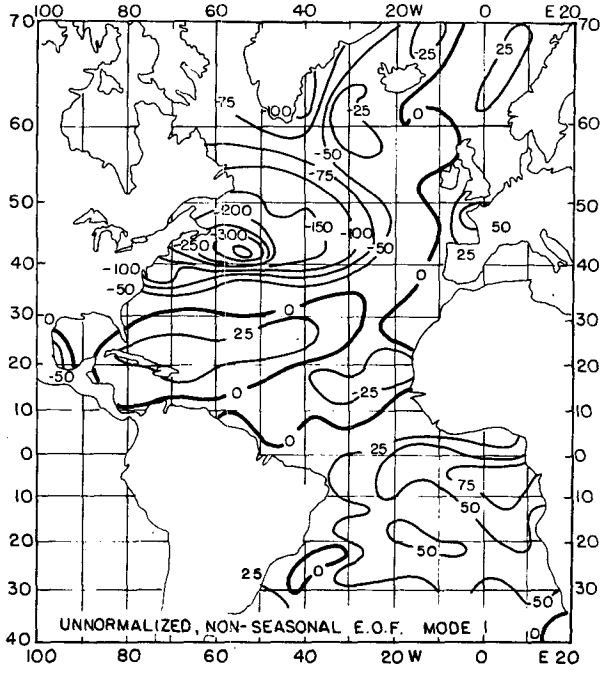

FIG. 4. Spatial pattern of the first principal component (mode 1) of the EOF representation of Atlantic Ocean SST anomalies. Contours have been multiplied by 1000.

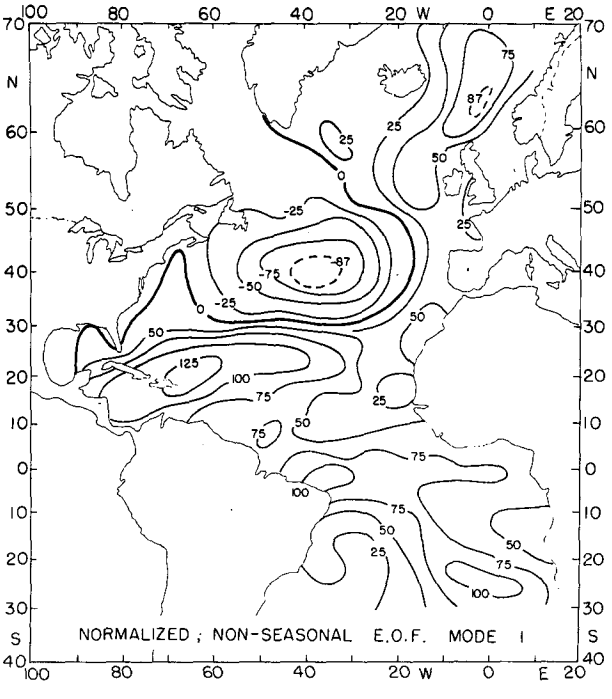

FIG. 5. Spatial pattern of the first principal component (mode 1) of the EOF representation of Atlantic Ocean nonseasonal SST anomalies normalized by the 1949–69 standard deviation for each 5° × 5° grid square.

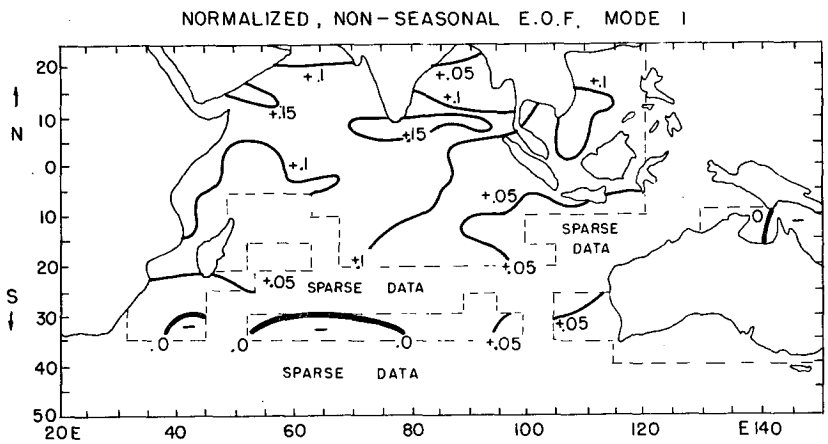

FIG. 6. Spatial pattern of the first principal component (mode 1) of the EOF representation of Indian Ocean nonseasonal SST anomalies normalized by its 1949–72 standard deviation for each calendar month for each 5° × 5° grid square.

4. Discussion

Our use of multiple regression in this investigation has advantages for the development of statistical prediction procedures. It also clearly brings out the lead-lag relationships between dependent and independent variables, and the sensitivity of the dependent variable to the individual independent variables, which may be helpful in the formulation of conceptual theories and models.

Regression equations (2), (3) and (4) indicate the sensitivities of the tropical, the extratropical Northern Hemisphere, and Southern Hemisphere tropospheric temperatures to oceanic SST's and aerosol concentrations over the northern tropics and over the Southern Hemisphere midlatitudes. Note in Eq. (3) that the Indian Ocean (I) and aerosol concentration over Mauna Loa (M) are not significant predictors for Northern Hemisphere extratropical tropospheric temperatures (NTT). The Aspendale dust index (AD) adds only marginal predictive power in (3). While it is difficult to see detailed correspondence between our findings and the results of Rowntree's (1972, 1976a,b, 1979) investigation using general circulation models of the effects of oceanic SST changes on surface pressure anomalies in the atmosphere, our results give evidence of the local and immediate effects of large-scale air-sea interactions as well as the Pacific Ocean teleconnections that he found. In agreement with Rowntree, we found the dominant effect of the tropical Pacific and Indian Ocean SST's on tropical tropospheric temperatures.

An increase in M and a decrease in AD both mean an increase in aerosol concentration, principally residing in the stratosphere (see, e.g., Meinel and Meinel, 1967; Newell, 1970). Our results show that increased aerosol concentrations lead to a drop in global tropospheric temperatures, in accord with observational findings of Newell and Weare (1976) and the modelling results of Hansen *et al.* (1978).

Eq. (4) seems to imply that Southern Hemisphere

TABLE 2. Correlations among variables in the regression equations.

a. For tropical tropospheric temperatures (TTT)

March 1958–December 1972

	TTT_t	P_{t-6}	A_t	I_{t-1}	M_t	AD_{t-2}
TTT_t	1.000					
P_{t-6}	0.599	1.000				
A_t	0.545	0.397	1.000			
I_{t-1}	0.556	0.543	0.310	1.000		
M_t	0.255	0.028	0.215	−0.053	1.000	
AD_{t-2}	−0.299	−0.139	−0.145	−0.037	−0.425	1.000

b. For Northern Hemisphere extratropical tropospheric temperatures (NTT)

February 1958–December 1972

	NTT_t	A_{t-9}	P_{t+4}	I_{t-12}	AD_{t-1}
NTT_t	1.000				
A_{t-9}	0.419	1.000			
P_{t+4}	−0.178	−0.163	1.000		
I_{t-12}	−0.007	0.187	−0.185	1.000	
AD_{t-1}	−0.129	0.001	−0.148	−0.073	1.000

c. For Southern Hemisphere extratropical tropospheric temperatures (STT)

October 1958–December 1972

	STT_t	M_{t-9}	AU_t	P_{t-2}	AD_t	I_t
STT_t	1.000					
M_{t-9}	0.320	1.000				
AU_t	−0.234	−0.034	1.000			
P_{t-2}	0.196	−0.025	0.274	1.000		
AD_t	−0.286	−0.059	0.192	−0.040	1.000	
I_t	0.178	0.117	0.325	0.540	0.089	1.000

TABLE 3. Correlations among variables in the regression equations at zero lag for the period January 1958–December 1972.

	TTT	NTT	STT	I	P	AU	A	M	AD
TTT	1.000								
NTT	0.319	1.000							
STT	0.297	0.175	1.000						
I	0.517	0.032	0.035	1.000					
P	0.395	−0.047	0.140	0.441	1.000				
AU	0.004	−0.245	−0.227	0.110	0.235	1.000			
A	0.545	0.226	0.093	0.285	0.318	0.461	1.000		
M	0.264	0.163	0.316	0.004	0.088	−0.130	0.218	1.000	
AD	−0.292	−0.118	−0.288	−0.082	−0.147	0.190	−0.141	−0.388	1.000

extratropical aerosol concentration (AD) affects Northern Hemisphere tropospheric temperature (NTT). However, a more likely interpretation is that aerosol concentrations over the Northern Hemisphere extratropical stratosphere directly affect NTT; that variations in this Northern Hemisphere aerosol concentration are highly correlated with variations in AD; and that AD functions like a proxy time series for the Northern Hemisphere extratropical aerosol concentration in Eq. (3). Aerosol over Mauna Loa (M) in the northern subtropics does not seem to significantly affect NTT. This hypothesis suggests a need for a Northern Hemisphere extratropical station to monitor aerosol concentrations.

By comparing correlation coefficients listed under the first columns of Tables 2a–2c with coefficients under corresponding columns of Table 3, one can see the improvement in the correlations for some variables when lags other than zero are used. In the absence of physical arguments to the contrary, the improvement is an indication that the regression involves that lag.

The strong serial correlation in the residuals which we obtain after using ordinary least-squares (OLS) procedures to estimate the coefficients of our regression equations suggests that there remain significant climatic processes not yet included in our regression models (see the Appendix). The importance of using generalized least-squares (GLS) procedures with our set of variables can be appreciated by comparing the estimates of variance of the dependent variable explained by the fitted values (right-hand side of the regression equations). In the case of the Southern Hemisphere extratropical tropospheric temperatures STT in equation (4), the ordinary least-squares-regression equation (which gives highly correlated residuals) appears to explain 29.2% of its variance, while the generalized least-squares-regression equation (which gives uncorrelated residuals and more precise estimates) yields the 21.8% estimate for the variance explained.

The relationship between sea and air temperature in the tropics is one that has been studied for many years, since the early work by Walker (1923, 1924) on the Southern Oscillation. Walker found that high pressure in the southeast Pacific was accompanied by low pressure over the Indian Ocean. It has long been recognized that higher pressures over the southeast Pacific are usually accompanied by colder SST's in the eastern tropical Pacific. The present analysis suggests that these lower SST's are accompanied by lower SST's in the Indian Ocean and cooler tropical mean tropospheric temperatures. One hypothesis unifying these observations is that the ocean temperatures of the eastern tropical Pacific are controlled by variations in zonal wind stress, with stronger winds corresponding to more upwelling along the equator and therefore colder surface waters. A decrease in equatorial SST's is associated with an increase of pressure in the southeast Pacific and a concomitant decrease in the pressure over the Indian Ocean. Lower pressures in the tropical Indian Ocean would be accompanied by increased convergence and cloudiness, which, in turn, would tend to reduce the ocean surface temperature. The reverse conditions would apply for warmer than normal eastern tropical Pacific Ocean temperatures.

From the point of view of climate forecasting, or as it was termed by Walker, foreshadowing, the importance of the Indian Ocean is unfortunate in that a six-year gap from 1973 to 1978 in the available analyzed values of Indian Ocean SST's cannot be filled at present. The forecasting skill attainable by means of a regression equation with no Indian Ocean SST's as predictor will probably be significantly less than optimum, at least for predicting tropical tropospheric temperatures. However, prediction of the tropospheric mean temperature is only one of our goals; the other is to understand the physical reasons for the observed interrelationships.

Acknowledgments. We are grateful to Dr. A. J. Dyer for aerosol data from Aspendale and to Dr. R. Hoffman for help in the analysis of the Atlantic Ocean data. The Mauna Loa transmission data were obtained from the Geophysical Monitoring for Climatic Change Program in the Air Resources Laboratory of NOAA, Boulder, Colorado. The research reported in this paper was supported by the

Department of Energy and by the Climate Dynamics Research Section of the National Science Foundation.

APPENDIX

Long Autocorrelations and GLS Regression Models

We discuss some statistical issues here such as the effects of a large or small number of predictors, the uses of ordinary least-squares (OLS) and generalized least-squares (GLS) procedures, conditions for the validity of estimates of standard errors, t-statistics and fraction of variance explained, and the significance levels of our regression coefficients.

We wanted to minimize the number of predictors because, in finite length data sets, the predictability of a predictand is a function of the ratio of the number of data points to the number of predictors: the greater this ratio, the less the artificial predictability introduced [for a discussion see Davis, (1976)]. On the other hand, we may not limit the number of predictands arbitrarily because omitting a true predictor introduces bias into our estimates of the regression coefficients. If this omitted true predictor has a long autocorrelation, this autocorrelation may result in serial correlation among the residuals E in Eq. (1), i.e., the value of the predictand minus the fitted value given by the right-hand side of the regression equation.

The Gauss-Markov theorem (e.g., Goldberger, 1964) states that the least squares method yields linear unbiased estimators which have minimum variance compared to other linear unbiased estimators. Unfortunately, OLS estimates of regression coefficients lose the least-variance property when the residuals are serially correlated. Hence, when we omit true predictors we degrade both the accuracy and precision of OLS estimates for the regression coefficients. Another common result of serially correlated residuals is that the OLS estimate of the fraction of variance of the predictand explained by the estimated regression equation is inflated to an unknown degree. Furthermore, the OLS estimates of the standard errors of the coefficients and their t statistics would then be incorrect.

Our procedure was to use initially an OLS method to obtain preliminary estimates of the regression coefficients and the corresponding residual time series. We then checked to see if we jeopardized the validity of our estimates by violating the assumptions underlying the Gauss-Markov theorem. We found a violation of the assumption that the expectation matrix of the error variance-covariance matrix be $\sigma^2\mathbf{I}$,where σ is the standard deviation of the errors and $\mathbf{I}$ the identity (diagonal) matrix of order equal to the length of the time series. This means that the error variance must be constant and the covariances must vanish, i.e., the error terms must have no serial correlation. The violation was revealed by the fact that the Durbin-Watson statistic (see, e.g., Johnston, 1972) had values sufficiently different from 2.00 to indicate the presence of substantial serial correlation among the residuals.

We then resorted to a GLS procedure described by Eisner and Pindyk (1973), which consists of a transformation of all the variables depending on the type of residual series, followed by an OLS estimation. The appropriate transformation must make the error matrix diagonal. We determined the appropriate transformation by an iterative procedure. First, we hypothesized that the residual series was an autoregressive series of first order such that the residual term at time t was given by

$$E_t = \rho E_{t-1} + \epsilon_t, \tag{5}$$

where the ϵ's are serially uncorrelated random terms. We next rearranged the regression equation (1) so that the new residual term, if our initial guess were correct, would be a random series of uncorrelated terms. We followed an iterative search procedure to find the value of ρ which would minimize the least-squares errors. We then applied an OLS procedure to obtain a set of regression coefficients and a corresponding residual time series. We tested our hypothesis regarding the form of the residual series by calculating the Durbin-Watson statistic to see if no substantial serial correlation in the residuals remained. We next assumed a second-order autoregressive form for the residuals such as

$$E_t = \rho_1 E_{t-1} + \rho_2 E_{t-2} + \epsilon_t. \tag{6}$$

We rearranged the regression equation accordingly, iterated for ρ_1 and ρ_2 (the two autoregression parameters), and ran an OLS estimation on the resulting equation, computed the fraction of variance explained, and the Durbin-Watson statistic for the residual series. Next we assumed the errors formed a first-order moving-average series with an initial guess for the moving-average parameter ρ such that the error term at time t was given by

$$E_t = \epsilon_t + \rho\epsilon_{t-1}, \tag{7}$$

where the ϵ's are serially uncorrelated random terms. Again we computed an OLS estimate for the regression coefficients, fraction of variance explained, and the Durbin-Watson statistic for the residual time series. Finally, we assumed a second-order moving-average form for the residual terms such as

$$E_t = \epsilon_t + \rho_1\epsilon_{t-1} + \rho_2\epsilon_{t-2}. \tag{8}$$

Among those regression equations which no longer showed serial correlation in their residual series, we chose as our regression model that one which gave the maximum fraction of variance explained. This procedure may not always succeed in eliminating serial correlation in the residuals.

The validity of the estimates of standard errors of the regression coefficients, the t-statistics, and the fraction of the variance of the predictand explained by the regression equation depends on the normality of the probability distribution curve of residual terms. The larger the number of terms, the closer the distribution approaches the normal shape. We checked the shape of the distributions of residuals left by our GLS procedures and found them to be substantially normal.

The number of degrees of freedom used in the estimates for the standard errors and the t-statistics was the number of terms in the residual series (which now were uncorrelated) minus the number of regression coefficients estimated increased by one. Thus, we avoided the need to estimate the reduction in the number of degrees of freedom appropriate for our predictor time series with long autocorrelations.

As a further check on the significance of our results (on the suggestion of an anonymous reviewer), we compared them with the regression equation estimated for the case when the dependent variable was put in reverse order. We went through the lead-lag selection process exactly as we did for the original series. Thus our "nonsense" series preserved the autocorrelation and other statistical properties of our original dependent variable. The resulting explanation of variance went down from 50.2 to 8.9% for TTT.

REFERENCES

Angell, J. K., and J. Korshover, 1975: Estimate of the global change in tropospheric temperature between 1958 and 1973. *Mon. Wea. Rev.*, **103**, 1007–1012.

Billing, C., 1979: Statistical predictability of Pacific Ocean surface temperature anomalies. M.S. thesis, Dept. of Meteor., MIT, 82 pp.

Davis, R. E., 1976: Predictability of sea surface temperature and sea level pressure anomalies over the North Pacific Ocean. *J. Phys. Oceanogr.*, **6**, 249–266.

Dyer, A. J., 1974: The effect of volcanic eruptions on global turbidity, and an attempt to detect long-term trends due to man. *Quart. J. Roy. Meteor. Soc.*, **100**, 563–571.

Eisner, M., and R. S. Pindyck, 1973: A generalized approach to estimation as implemented in the TROLL/1 system. *Ann. Econ. Social Measure.*, **2**, No. 1, 29–51.

Goldberger, A. S., 1964: *Econometric Theory*. Wiley, 410 pp.

Hansen, J. E., W. C. Wang and A. A. Lacis, 1978: Mount Agung eruption provides test of a global climatic perturbation. *Science*, **199**, 1065.

Hsiung, Jane Cheng, 1978: Statistical prediction of Atlantic sea-surface temperature using empirical orthogonal functions. M.S. thesis, MIT, 80 pp.

Johnston, J., 1972: *Econometric Methods*, 2nd ed. McGraw-Hill, 447 pp.

Kutzbach, J. E., 1967: Empirical eigenvectors of sea-level pressure, surface temperature and precipitation complexes over North America. *J. Appl. Meteor.*, **6**, 791–802.

Meinel, A. B., and M. P. Meinel, 1967: Volcanic sunset-glow stratum: origin. *Science*, **155**, 189.

National Oceanic and Atmospheric Administration, 1958–1972: *Monthly Climatic Data for the World*, Vols. 11–31.

Newell, R. E., 1970: Modification of stratospheric properties by trace constituent changes. *Nature*, **227**, 697–699.

——, and B. C. Weare, 1976: Factors governing tropospheric mean temperature. *Science*, **194**, 1413–1414.

——, A. R. Navato and J. Hsiung, 1978: Long-term global sea surface temperature fluctuations and their possible influence on atmospheric CO_2 concentrations. *Pure Appl. Geophys.*, **116**, 351–371.

Pueschel, R. F., L. Machta, G. F. Cotton, E. C. Flowers and J. T. Peterson, 1972: Normal incidence radiation trends on Mauna Loa, Hawaii. *Nature*, **240**, 545–547.

Ramage, C. S., F. R. Miller, and C. Jefferies, 1972: *Meteorological Atlas of the International Indian Ocean Expedition: The Surface Climate of 1963 and 1964*, Vol. 1. U.S. Govt. Printing Office, 169 pp.

Rowntree, P. R., 1972: The influence of tropical east Pacific Ocean temperatures on the atmosphere. *Quart. J. Roy. Meteor. Soc.*, **98**, 290–321.

——, 1979: The effects of changes in ocean temperature on the atmosphere. *Dyn. Atmos. Oceans*, **3**, 373–390.

——, 1976a: Response of the atmosphere to a tropical Atlantic Ocean temperature anomaly. *Quart. J. Roy. Meteor. Soc.*, **102**, 607–625.

——, 1976b: Tropical forcing of atmospheric motions in a numerical model. *Quart. J. Roy. Meteor. Soc.*, **102**, 583–605.

Royal Netherlands Meteorological Institute, 1976: *Marine Climatological Summaries for the Mediterranean and Southern Indian Ocean*, Vols. 2–7.

Walker, G. T., 1923: Correlation in seasonal variations of weather, VIII. A preliminary study of world weather. *India Meteor. Dept. Mem.*, **24**, 75–131.

——, 1924: Correlation in seasonal variations of weather, IX. A further study of world weather. *India Meteor. Dept. Mem.*, **24**, 275–332.

Weare, B. C., 1977: Empirical orthogonal analysis of Atlantic Ocean surface temperatures. *Quart. J. Roy. Meteor. Soc.*, **103**, 467–478.

——, 1979: A statistical study of the relationships between ocean surface temperatures and the Indian monsoon. *J. Atmos. Sci.*, **36**, 2279–2291.

——, A. R. Navato and R. E. Newell, 1976: Empirical orthogonal analysis of Pacific sea surface temperatures. *J. Phys. Oceanogr.*, **6**, 671–678.